WORLD CONFERENCE ON TIMBER ENGINEERING 2025
BRISBANE, AUSTRALIA
Advancing Timber for the Future Built Environment

FIRE BEHAVIOUR OF CLT FLOOR TO WALL CONNECTIONS: FINDINGS FROM THE WOODWISE PROJECT

Nicolas Coello[1], Erica C. Fischer[2], Laura Hasburgh[3], David Barber[4], Kara Yedinak[5], Ines Pitari[6]

ABSTRACT: Cross-laminated timber (CLT) is increasingly used in multi-story construction due to its structural efficiency and sustainability. However, the fire performance of CLT floor-to-wall connections remains a critical concern, particularly in balloon-frame construction, where there are complex interactions between the steel and timber components and fire-induced degradation of both materials can compromise structural integrity. This study, part of the WOODWISE project, examines the fire behaviour of CLT floor-to-wall connections through large-scale compartment fire tests. The research evaluates the effects of connection configuration and encapsulation on char depth and charred area. Two connection types—exposed and concealed steel angle connections—were tested under fully exposed and fully encapsulated conditions. Results indicate that concealed steel angle connections exhibit greater char depth than exposed steel configuration. Comparison of measured char depths with prescriptive design standards indicated that actual charring can exceed values predicted by code standards, particularly in concealed steel angle connections and under more severe fire exposure scenarios. Encapsulation significantly reduces char propagation, highlighting its effectiveness in improving fire resistance. Additionally, compartment encapsulation influences fire dynamics, affecting heat exposure and char development. These findings contribute to the importance of connection detailing in exposed timber structures.

KEYWORDS: Mass timber, fire performance, timber connections.

1 – INTRODUCTION

Due to the panelised nature of Cross Laminated Timber (CLT), this material provides increased speed of assembly over conventional construction materials, such as steel and concrete. Multi-story walls can be erected and floors then dropped into place supported on a timber or steel ledger. This type of construction is called balloon-frame construction. Significant barriers remain in using CLT for balloon-frame construction, particularly concerning the stability of the building during a fire, both during the heating and decay phases of a fire. The study described within this paper is part of a comprehensive project, WOODWISE (Wood Optimization for Occupant safety, Design Innovation, Wood Engineering, Smouldering, and Emissions), which aims to advance the understanding on the behaviour of mass timber structures in fire and the fire dynamics within mass timber structures.

Timber balloon-frame floor-to-wall connections have been widely studied through mid-scale furnace standard tests [1]. The results of these tests demonstrated that steel elements can cause excessive temperature rise in nonexposed surfaces and that thermal penetration through the connection continues in timber even after peak fire temperatures [5]. Future work within the WOODWISE project will include comparing the findings presented in this paper with results obtained from standard fire tests conducted in the past.

While some large-scale compartment fire tests have included balloon-frame connections [4], data on thermal penetrations and char depths were not collected. In addition, these tests did not include a decay phase of the fire. However, it has been mentioned that smouldering hotspots can develop around connections during the decay phase of a fire, particularly along the edges of slabs and at floor-to-wall connections. These hotspots can lead either to reignition or to localised loss of strength and stiffness of the timber potentially compromising the stability of the structure [6].

To fill these identified gaps in knowledge, the authors performed a series of large-scale compartment fire tests

[1] Nicolas Coello, School of Civil and Construction Engineering, Oregon State University, Corvallis, Oregon, United States, coelloce@oregonstate.edu
[2] Erica Fischer Ph.D., P.E., School of Civil and Construction Engineering, Oregon State University, Corvallis, Oregon, United States, erica.fischer@oregonstate.edu
[3] Laura Hasburgh Ph.D., P.E., Forest Products Laboratory, United States Forest Service, Madison, Wisconsin, United States, laura.e.hasburgh@usda.gov
[4] David Barber P.Eng., CPEng., Fire Protection Engineering, Arup, Washington, D.C., United States, david.barber@arup.com
[5] Kara Yedinak Ph.D., Northern Research Station, United States Forest Service, Madison, Wisconsin, United States, kara.yedinak@usda.gov
[6] Ines Pitari, School of Civil and Construction Engineering, Oregon State University, Corvallis, Oregon, United States, pitarii@oregonstate.edu

https://doi.org/10.52202/080513-0130

as a part of the WOODWISE project. The objectives of this study are to:

1. Evaluate the influence of balloon-frame connection configuration on char propagation when exposed to natural fires.
2. Assess the effectiveness of encapsulation on preventing char propagation for two types of balloon-frame connections when exposed to natural fires.
3. Compare experimental char depth measurements with prescriptive design char depths from standard fire design codes.

The data used to achieve these objectives include temperature recordings and post-test sample analysis. The key parameters for comparing connection configurations and effectiveness of encapsulation are char depth and charred area of the connection section.

2 – TEST SETUP

This study compares two compartment fire tests as a part of the WOODWISE research project. An overview of the entire testing program is provided in [7]. Test #2 and Test #3 are two compartments with different non-combustible encapsulation designs. The large-scale tests were conducted at the Bureau of Alcohol, Tobacco, Firearms and Explosives (ATF) Fire Research Laboratory (FRL), located within the National Laboratory Center (NLC) in Beltsville, Maryland, United States. Each compartment had dimensions of 2.84 m wide by 5.89 m deep by 2.44 m high, and a single opening of 1.74 m wide by 1.87 m high, corresponding to an opening factor of 16.2 $m^{-1/2}$. The walls and ceiling were constructed of five-ply Southern Yellow Pine V2 CLT, while the glulam frame elements (two columns and one beam) were Spruce-Pine-Fir (Fig. 1).

The compartments discussed within this paper had a fuel load of 798 MJ/m^2 from residential furniture. Fig. 1 represents a general plan view of the large-scale compartment, including the location of the floor-to-wall connections analysed in the current study. Further details on the test setup and procedure can be found in [7].

2.1 ENCAPSULATION DETAILS

In both compartment tests (Test #2 and Test #3), 81% and 45%, respectively, of the total surface area was exposed mass timber. Test #2 had all CLT walls exposed, whereas in Test #3, the two side walls perpendicular to the compartment opening were encapsulated with two layers of 15.9 mm thickness Type-X gypsum board. Both encapsulation cases had the CLT ceiling, back wall, front wall, and the glulam frame exposed.

2.2 FLOOR-TO-WALL CONNECTIONS

Two different configurations of CLT balloon-frame floor-to-wall connections were installed at the back wall of the compartments. The compartment's ceiling panel was placed atop the walls, forming a platform-framed connection. A CLT piece, noted as a “dummy block”,

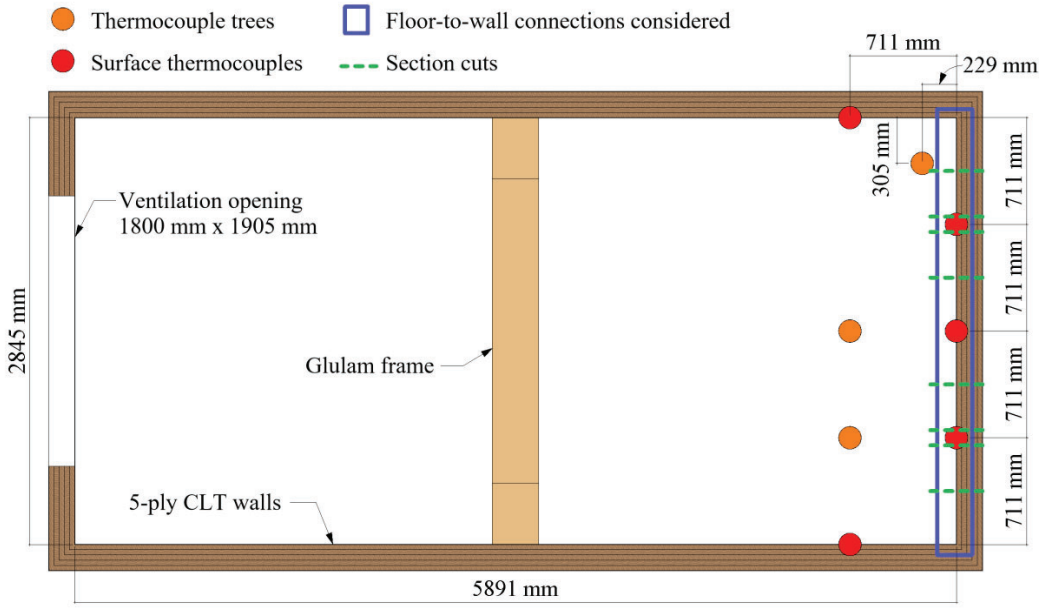

Figure 1. Plan view of typical large-scale compartment. Not all sensors shown for clarity.

https://doi.org/10.52202/080513-0130

was attached to the back wall through balloon-frame connections leaving a gap between the “dummy block” and the compartment's ceiling panel. This detail ensured that the potential failure of the balloon-frame test connections would not cause a fire integrity failure of the compartment.

In the following sections, ‘floor-to-wall connections’ refers exclusively to the balloon-frame connections. Each connection consisted of an A36 steel angle with dimensions 152 mm x 101 mm x 9.5 mm. Simpson Strong-Tie® SDWS™ 127 mm timber screws spaced 304.8 mm apart, secured the steel angle to the CLT wall and “dummy block”.

Two configurations of the floor-to-wall connection were tested: an exposed steel angle (ES) and a concealed steel angle (CS). The exposed steel angle had the long leg of the steel angle attached to the back wall of the compartment below the dummy block making it visible from the interior of the compartment. The concealed steel angle had the long leg of the steel angle attached to the back wall of the compartment behind the dummy block, thereby hidden within the floor-wall joint, with the dummy block notched to accommodate the steel angle leg. The construction process is represented in Fig. 2, which visually illustrates key stages of both ES and CS connections, including steel angle placement, dummy block positioning, and the finished connections.

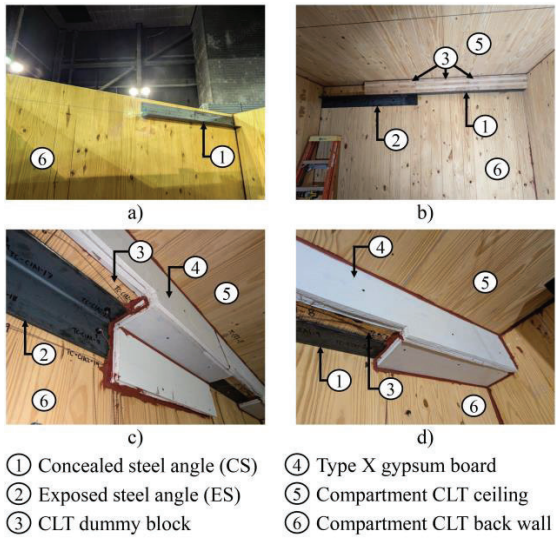

Figure 2. Construction stages of floor-to-wall connections. a) Placement of the concealed steel angle (CS) before installing the compartment ceiling; b) Installation of the CLT dummy block; c) Completed configuration of ES; d) Completed configuration of CS.

Each configuration was tested under two encapsulation conditions: fully exposed connection (no encapsulation) (FEX) and fully encapsulated connection (FEN), where the steel angle was protected by two layers of 15.9 mm Type-X gypsum board. Across all four tested cases, three layers of gypsum board were attached to the face of the dummy block facing the interior of the compartment to simulate a continuous panel. Each tested floor-to-wall connection segment was 711 mm long. Fig. 3 presents an elevation view of the back wall in Test #2, identifying the four floor-to-wall connection cases:

FEX-ES: Fully exposed, exposed steel angle;

FEN-ES: Fully encapsulated, exposed steel angle;

FEX-CS: Fully exposed, concealed steel angle;

FEN-CS: Fully encapsulated, concealed steel angle.

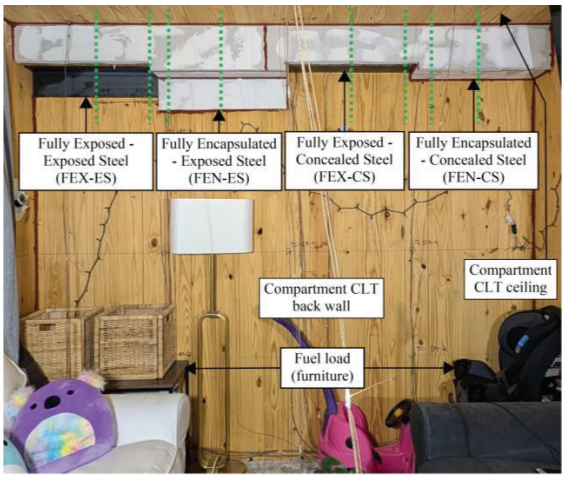

Figure 3. Elevation view of the balloon-frame connections tested. Green dashed lines represent the post-test cut locations.

The encapsulation layers appear as white gypsum board panels surrounding the steel angles. The compartment CLT back wall and ceiling are labelled for spatial reference. Additionally, the fuel load (furniture) is marked to indicate its proximity to the connections.

Each assembly scheme incorporated HILTI® FS-ONE MAX™ fire block sealant at the joints between gypsum boards and between the gypsum board and timber. The fire block sealant was intended to prevent heat penetration through the joints, thereby reducing the risk of early failure.

2.3 FIRE DEMAND

Gas temperatures measured within 711 mm of the floor-to-wall connections provide insight into the fire demand on the connections (Fig. 1). Fig. 4 presents the range of temperatures recorded by surface thermocouples (TC) and thermocouple trees (TCT) at the rear of the compartment during each test. The fire duration was approximately 95 minutes for Test #2 and 107 minutes

https://doi.org/10.52202/080513-0130

for Test #3, with peak mean temperatures reaching 987 °C and 993 °C, for Tests #2 and #3, respectively. Although the peak mean temperatures were similar, it is notable that Test #3 exhibited consistently higher temperatures during the first 60 minutes.

Due to the longer duration and higher temperatures at the rear of the compartment in Test #3 compared to Test #2, greater char depths are anticipated. Consequently, direct comparisons between Tests #2 and #3 will require additional data processing and analysis.

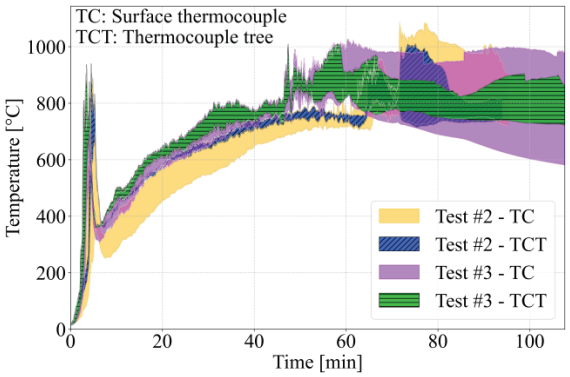

Figure 4. Fire exposure of floor-to-wall connections.

2.4 INSTRUMENTATION

Type K thermocouples were placed at the surface of the connection and embedded within the CLT back wall and dummy block to measure temperatures at steel and timber surfaces, steel-timber interfaces, and various depths within the CLT near the screws. Fig. 5 illustrates the placement of surface thermocouples (blue circles) on the steel angle and the CLT surface of both the compartment back wall and the dummy block. Embedded thermocouples (green circles) were inserted into the dummy block from the unexposed side, positioned 25.4 mm from the screws either in-plane (parallel to the screw, as shown in Fig. 5) or out-of-plane (perpendicular to the plane shown in Fig. 5). These thermocouples were embedded at depths ranging from 0 mm to 127 mm deep from the exposed surface.

Char depths were calculated from the recorded temperatures based on the thermocouple embedment depths and the 300 °C isotherm [8]. To distinguish the computed char depth from the physically measured char depth, the term ‘thermocouple-derived char depth’ will be used in the following sections to refer specifically to the computed values.

Additionally, thermocouple trees were placed throughout the compartment to measure gas temperatures at different heights. Fig. 1 shows only the thermocouple tress within the proximity of the connections. A full plan view of the locations of all thermocouple trees is provided within [7].

3 –RESULTS

This section presents the measured and computed char depths, charred areas, and temperature variations for the different configurations of floor-to-wall connections. Post-test images and binary figures illustrate the extent of charring, while quantitative measurements provide a basis for comparison. The portion of the connection considered in this study is the CLT piece used to simulate the floor panel or “dummy block”.

3.1 CHAR DEPTH

Each connection presented in Section 2.2 was analysed through cross-sectional cuts made at locations along the CLT dummy block. Two cuts per connection were made at the locations shown in Fig. 1 and Fig. 3, and four measurements of char depth and char area were taken per cut. Fig. 6 and Fig. 7 illustrate the connection configurations and encapsulation conditions considered in this study, as well as the location of the physical measurements taken on each post-test cut. The comparison between fully exposed and encapsulated connections reveals a significant difference in char depth. In both Test #2 and Test #3, the fully exposed connections (FEX-EX and FEX-CS) experienced substantially greater charring than their encapsulated counterparts (FEN-EX and FEN-CS). These results highlight the effectiveness of encapsulation in reducing char depth, as it limits the exposure.

Table 1 and Table 2 show the average vertical char depth of fully exposed (FEX) and fully encapsulated (FEN) connections, respectively. The reduction in char depth due to encapsulation is more pronounced in Test #2, where FEN-EX and FEN-CS exhibited only 29% and 37% of the char depth observed in FEX-EX and FEX-CS, respectively. In Test #3, encapsulation still played a protective role, reducing char depth to 51% and 73% of the values recorded in the fully exposed connections.

https://doi.org/10.52202/080513-0130

For the fully exposed connections, FEX-CS (concealed steel angle) consistently exhibited a greater char depth compared to FEX-EX (exposed steel angle). The concealed steel angle connections showed an increased char depth relative to the exposed steel angle by 21.9 mm in Test #2 and 12.3 mm in Test #3, indicating that steel angle orientation significantly influenced charring. A similar trend was observed for the encapsulated connections, where char depths for FEN-CS (concealed steel angle) were also larger than FEN-EX (exposed steel angle), by 11.9 mm in Test #2 and 25.2 mm in Test #3. This suggests the concealed angle configuration contributes to deeper char formation, even under fully encapsulated conditions. The differences observed can be explained by considering that the steel angle heats uniformly due to its high thermal conductivity; although the exposed angle initially heats faster, prolonged exposure results in similar temperatures for both configurations. The critical distinction lies in the contact area with the timber section analysed in this paper (i.e. dummy block): the concealed angle has two heated steel surfaces contacting the dummy block, whereas the exposed angle has only one. This increased contact area significantly intensifies the heat exposure of the timber,

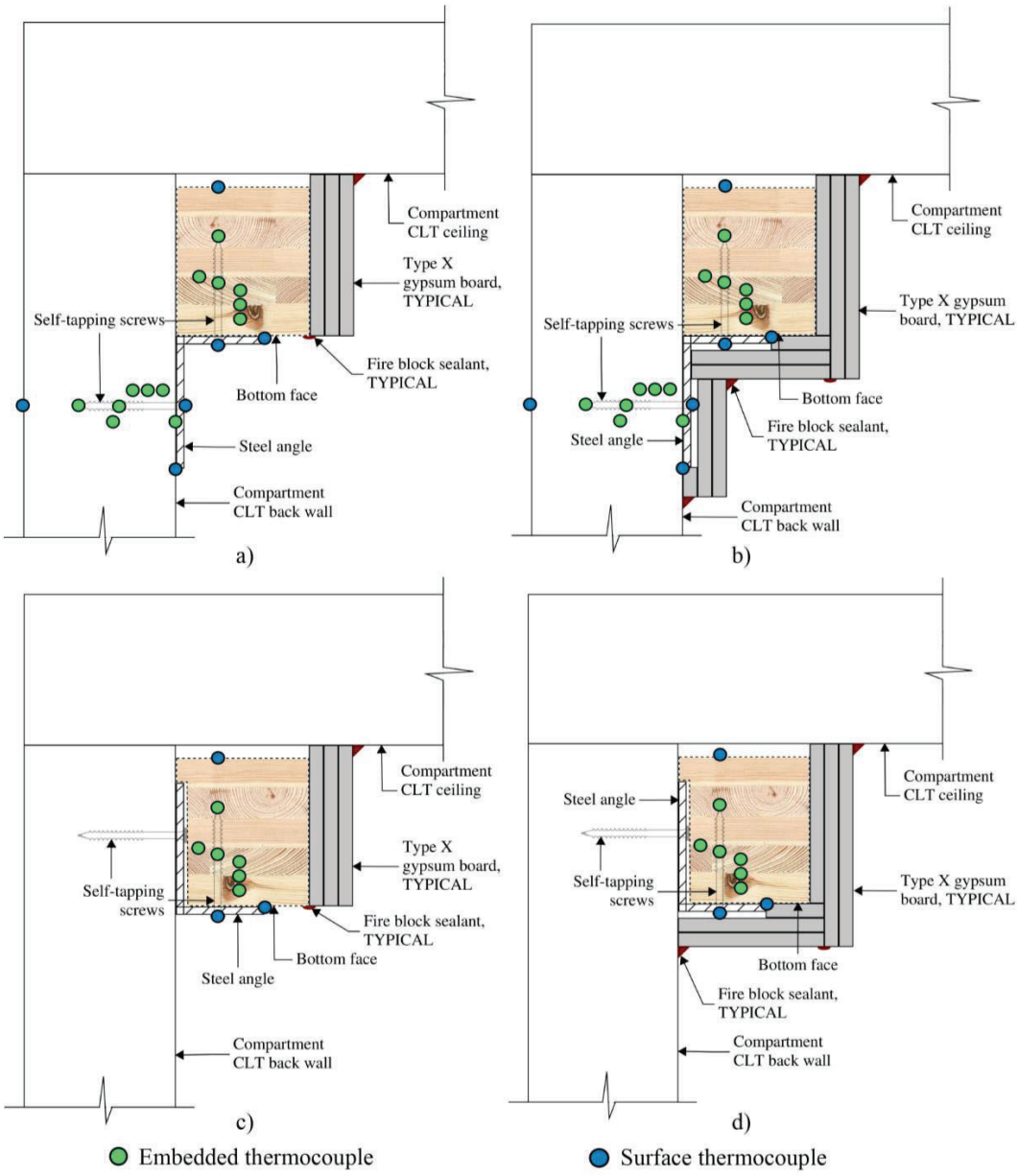

Figure 5. As-built assembly scheme of the floor-to-wall connections tested. a) FEX-ES; b) FEN-ES; c) FEX-CS; d) FEN-CS.

https://doi.org/10.52202/080513-0130

leading to the consistently greater char depths measured in concealed angle configurations.

Test #2, which had no encapsulation on the compartment walls, generally exhibited lower char depths than Test #3, which had partially encapsulated walls. This is consistent with observations that the fire during Test #2 was less severe compared to Test #3, which had a longer duration fire with higher temperatures, particularly during the first 60 minutes of testing. The increase in char depth between Test #2 and Test #3 was observed in both fully exposed connections and encapsulated connections. For the fully exposed connections, char depths for FEX-EX were 64% greater than for Test #2 (from 44.5 mm to 73.2 mm), while char depths for FEX-CS were 29% greater (from 66.4 mm to 85.5 mm). The fully encapsulated connections also displayed a substantial rise in char depth, with the char depths for FEN-EX increasing by 194% (from 12.7 mm to 37.3 mm) and the char depths for FEN-CS by 154% (from 24.6 mm to 62.5 mm. As shown in Fig. 4, the fire during Test #3 exhibited consistently higher temperatures throughout most of the test duration, contributing to greater char depths. Therefore, the differences in char depths between Tests #2 and #3 reflect expected outcomes due to the varying severity of the fires.

Despite the overall increase in char depth from Test #2 to Test #3, encapsulated connections in both tests continued to exhibit significantly lower char depths than their fully exposed counterparts, highlighting the role of encapsulation in slowing thermal propagation.

In addition to physical measurements from post-test cuts, temperature data recorded by embedded and surface thermocouples were used to estimate char depths. The thermocouple-derived measurements, included in Tables 1 and 2, generally followed the same trends observed in

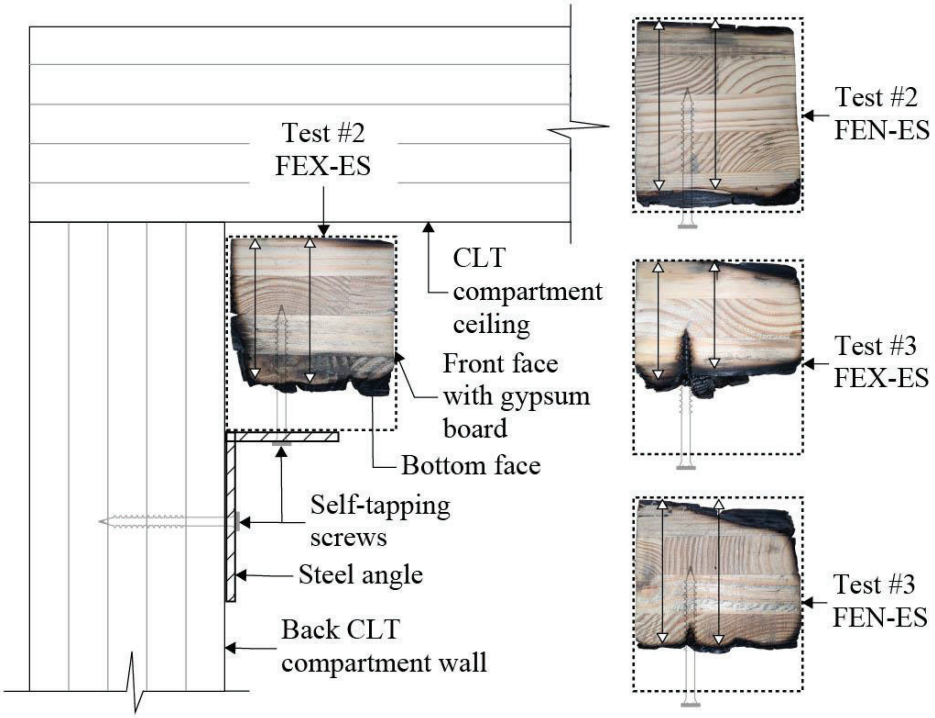

Figure 6. Charred section cuts. Exposed steel connection. White arrows represent locations where measurements were taken.

Table 1. Char depth in fully exposed connections.

Test	Connection configuration	Char depth [mm]					
		Post-test measurement		Thermocouple-derived		Eurocode 5 [11]	NDS [12]
		Mean	Standard error	Mean	Standard error		
Test #2	FEX-ES	44.5	0.7	31.3	2.2	66.7	60.5
	FEX-CS	66.4	4.1	36.9	5.2		
Test #3	FEX-ES	73.2	1.7	54.3	4.1	75.4	68.4
	FEX-CS	85.5	4.6	63.4	7.3		

https://doi.org/10.52202/080513-0130

post-test char depth measurements. However, char depth derived from thermocouples were consistently lower than those measured directly, particularly for fully exposed connections. For example, in Test #2, thermocouple-derived char depths for FEX-EX and FEX-CS were 31.4 mm and 37.0 mm, respectively, compared to post-test measurements of 44.5 mm and 66.4 mm. Similarly, in Test #3, thermocouple-derived char depths were 54.3 mm for FEX-EX and 63.4 mm for FEX-CS, compared to post-test values of 73.2 mm and 85.5 mm, respectively. This discrepancy arises because the wood continues to char even after temperatures drop below 300 °C, due to sustained transient heating and prolonged smouldering. The smouldering process, especially pronounced behind protective gypsum layers, continues for hours after extinguishing the fire, increasing the actual char depth beyond thermocouple-derived estimates. Despite these differences, the standard error values for both measurement methods remained within a similar range, though slightly higher for thermocouple-derived char depths. Increasing the number of thermocouples may help reduce this variation.

Post-test measurements of the fully exposed connections (FEX) were compared to prescriptive design char depths, which were calculated using standard charring rates from Eurocode 5 [11] and the National Design Specification (NDS) [12], along with the duration of each test. The Eurocode nominal char rate of 0.7 mm/min (not including the zero-stiffness layer) and the NDS char nominal char rate for CLT of 0.64 mm/min were both used to calculate char depths.

Measured char depths in Test #2 were smaller than those calculated with the Eurocode prescriptive char rate. Exposed steel (ES) connections had char depths 50%

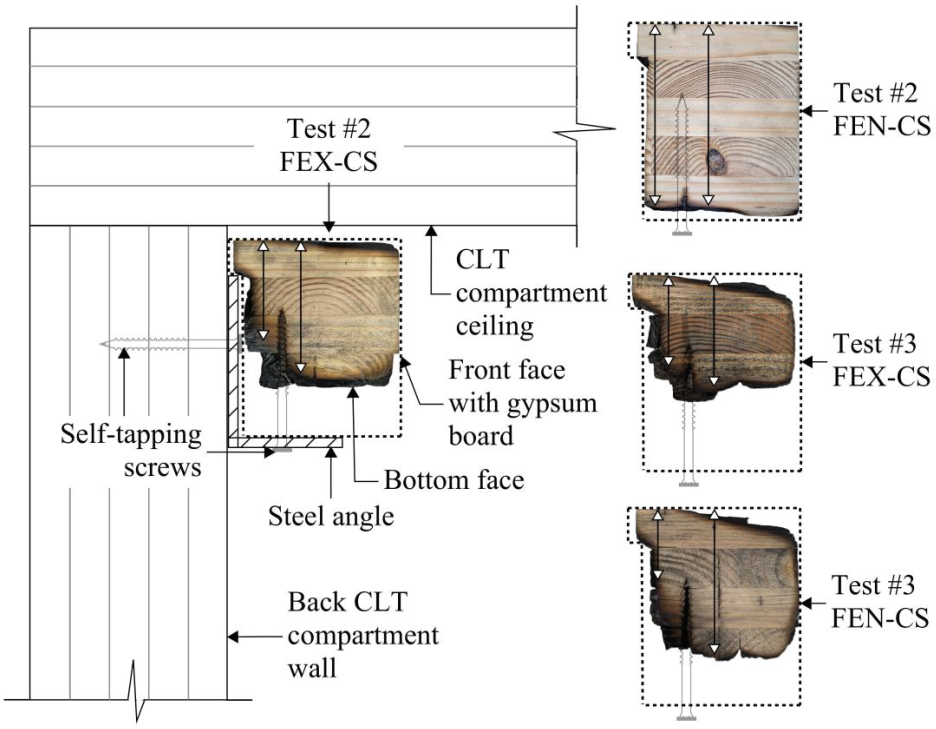

Figure 7. Charred section cuts. Concealed steel connection. White arrows represent locations where measurements were taken.

Table 2. Char depth in fully encapsulated connections.

Test	Connection configuration	Char depth [mm]			
		Post-test measurement		Thermocouple-derived	
		Mean	Standard error	Mean	Standard error
Test #2	FEN-ES	12.7	2.8	2.0	N/A*
	FEN-CS	24.6	5.7	26.6	0.2
Test #3	FEN-ES	37.3	1.6	33.8	4.1
	FEN-CS	62.5	10.4	30.3	3.7

*Only one sensor measured temperatures above 300 °C

https://doi.org/10.52202/080513-0130

below those calculated with the Eurocode char rate whereas concealed steel (CS) was less than 1% below. The char depth calculated using the NDS char rate was 36% higher than measured values for ES but 9% lower for CS connection configuration. In Test #3, the measured char depths for ES (73.2 mm) were 3% lower than those calculated with the Eurocode char rate (75.4 mm) but exceeded those calculated with the NDS char rate (68.4 mm) by 7%. Char depths for CS (85.5 mm) exceeded both those calculated using the Eurocode and the NDS char rates, by 12% and 20% respectively. These discrepancies highlight that the prescriptive char rates may underestimate char propagation in natural fires, especially for concealed steel configurations or more severe fire exposures, as observed in Test #3.

For encapsulated connections, thermocouple-derived char depths were closer to post-test measurements, with FEN-EX in Test #2 showing a particularly large deviation (2.1 mm from thermocouples vs. 12.7 mm post-test), while other configurations showed better agreement. The smaller char depths measured by thermocouples may be attributed to transient heating and smouldering occurring below the 300°C threshold, which thermocouples do not capture. In contrast, physical measurements were taken up to the point of visible discoloration. Additionally, discrepancies between measured and thermocouple-derived char depths could also result from human error during the physical measurement process.

Overall, the combination of physical measurements and thermocouple data confirms that encapsulation significantly reduces char depth. Additionally, the greater char depth observed in concealed steel connections, regardless of encapsulation, suggests the influence of connection configuration.

Temperature trends shown in Figures 8 and 9 provide further insights into fire exposure for the different connection configurations. In Test #2, surface temperature differences between the steel angle in ES and CS were not evident before 65 minutes into the test. Between 65 and 70 minutes, the surface temperature of the CS connection was higher than that of the ES connection, but after 70 minutes, the temperatures converged again. The temperature within the dummy blocks remained similar until about 80 minutes, at which point divergence was observed, with the ES connection exhibiting higher temperatures.

In Test #3, the steel surface temperature of the ES connection was initially higher than that of the CS connection up to 30 minutes into the test. After this point,

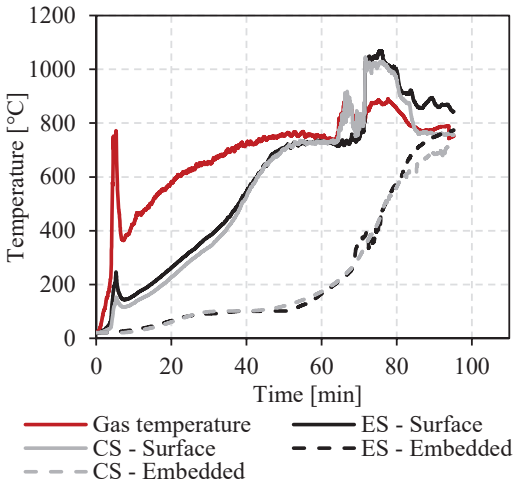

Figure 8. Temperatures comparison in Test #2

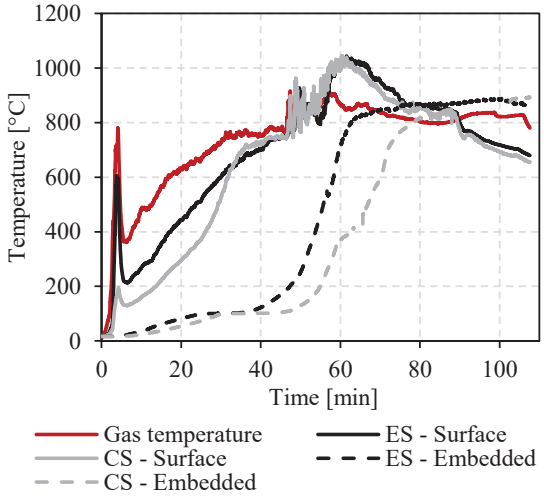

Figure 9. Temperatures comparison in Test #3

as compartment temperatures levelled off, the surface temperatures of both connections became similar (within 3.3% on average, with a standard error of 0.04%), further emphasizing the diminishing effect of the exposed steel area as the compartment reached thermal equilibrium. However, within the dummy blocks, the ES connection consistently exhibited higher temperatures than the CS connection throughout the test.

3.2 CHARRED AREA

The charred area was determined as a percentage of the original cross-sectional area of the dummy block (152 mm × 175 mm). This percentage was computed by processing images taken orthogonally to each post-test sample cut. The image processing followed a similar approach as described in [8], beginning with converting the original sample photo into a grayscale image.

https://doi.org/10.52202/080513-0130

A binary image was then generated using a threshold grey value of 50 to distinguish charred regions. To improve accuracy, manual corrections were applied to the binary images to eliminate misidentified charred areas. Finally, the corrected binary image was scaled to the original cross-section dimensions, and the percentage of black pixels in the image was used to quantify the charred area. Fig. 10 illustrates the image processing methodology, showing the transformation from the

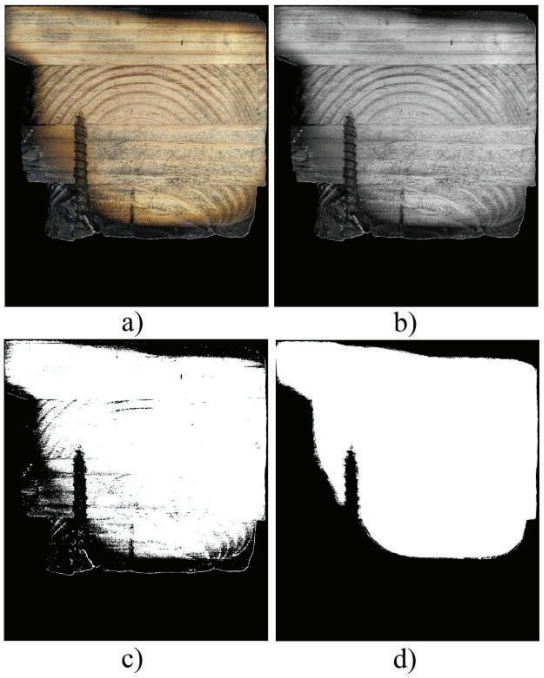

Figure 10. Charred area determination of Test #2 FEX-CS, charred area: 47%. a) Sample cut photo; b) Gray scale image; c) Binary image; d) Corrected binary image.

original sample cut photo to the corrected binary image used for analysis.

Table 3 shows the results for fully exposed connections. The charred area for the FEX-ES and FEX-CS configurations ranged from 30% to 61%, with consistently higher charred areas observed in Test #3 compared to Test #2. Additionally, FEX-CS connections exhibited more char than FEX-ES connections in both tests.

Table 3. Charred area in fully exposed connections.

Test	Connection configuration	Charred area [%]	
		Mean	Standard error
Test #2	FEX-ES	29.7%	0.7%
	FEX-CS	52.4%	5.0%
Test #3	FEX-ES	51.4%	2.3%
	FEX-CS	61.4%	0.4%

Table 4 presents the charred areas for fully encapsulated connections, which were significantly lower than those in the exposed condition. The charred area ranged from 12% to 41%, with FEN-CS configurations consistently exhibiting more char than FEN-EX configurations. Like the exposed connections, Test #3 resulted in higher charred areas than Test #2.

Table 4. Charred area in fully encapsulated connections.

Test	Connection configuration	Charred area [%]	
		Mean	Standard error
Test #2	FEN-ES	12.4%	1.7%
	FEN-CS	22.7%	5.8%
Test #3	FEN-ES	28.6%	4.5%
	FEN-CS	40.6%	3.7%

Table 5 highlights the comparative differences between exposed (ES) and concealed (CS) steel angle connections across both tests. Differences in char depth ranged from 19% to 50% in Test 2 and 0% to 34% in Test #3, while charred area differences varied between 24% and 55% in Test #2 and 8% to 24% in Test #3. These findings confirm that connection detailing significantly influences char depth, with concealed steel angles consistently exhibiting greater charring.

Table 5. Range of difference between ES and CS

Test	Char depth difference	Charred area difference
Test #2	19% - 50%	24% - 55%
Test #3	0% - 34%	8% - 24%

4 –CONCLUSIONS

This study evaluated the influence of CLT floor-to-wall connection configurations on char propagation when exposed to natural fires. The results demonstrated that char depths in concealed steel angle connections were larger compared to exposed steel angle connections. Encapsulation significantly mitigated this effect, with fully encapsulated connections experiencing substantially less char development. The difference in char depth and charred area between concealed steel and exposed steel configurations was more pronounced in fully exposed connections than in the encapsulated connections. These findings indicate that connection detailing plays a crucial role in determining fire performance.

Comparison of measured char depths with prescriptive design standards indicated that charring in these connections under natural fire exposure can significantly exceed predicted char depths using prescribed char rates

https://doi.org/10.52202/080513-0130

from standards. These prescribed char rates were developed for standard fire exposures. These results were particularly evident for concealed steel angle connections and when connections were exposed to more severe fire exposures. These findings underscore the need for char rates under natural fire exposures.

These results also confirm that connection encapsulation is an effective strategy for reducing char depth in fire-exposed mass timber connections regardless of compartment encapsulation. Future work includes comparing these results against standard fire tests and developing correlations to better understand connection behaviour under standard versus natural fire conditions.

5 – ACKNOWLEDGEMENT

This research was funded by the National Institute of Food and Agriculture. C-REEMS Grant Proposal Number: 2022-08935; and the USDA Agricultural Research Services. TDI Proposal Number: USDA ARS 58-0204-4-002.

The views expressed in this article are those of the author(s) and do not necessarily represent the views or policies of the U.S. Forest Service.

6 – REFERENCES

[1] A. Redus, “The Fundamental Behavior of CLT Floor-to-Wall Connections in Fire,” Oregon State University, 2022.

[2] M. Audebert, D. Dhima, A. Bouchaïr and N. Pinoteau, “Simplified Design Method for Fire Resistance of Timber Connections,” Journal of Structural Engineering, vol. 147, no. 12, 2021.

[3] J. Liu and E. Fischer, “Review of large-scale CLT compartment fire tests,” Construction and Building Materials, vol. 318, 2022.

[4] S. Zelinka, L. Hasburgh, K. Bourne, D. Tucholski and J. Oullette, “Compartment Fire Testing of a Two-Story Mass Timber Building,” U.S. Department of Agriculture, Madison, 2018.

[5] P. Horne, A. Abu, A. Palermo and P. Moss, “Thermal response of timber connections in the cooling phase,” Fire And Materials, vol. 47, no. 4, pp. 479-497, 2023.

[6] H. Mitchell, R. Amin, P. Kotsovinos, M. Heidari, D. Thomson, D. Barber and G. Rein, “Observations of smouldering fire in a large timber compartment,” in World Conference on Timber Engineering, Oslo, 2023.

[7] E. Fischer, I. Pitari, L. Hasburgh, D. Barber, K. Yedinak, A. Holder and N. Coello, “WOODWISE: Large-Scale Compartment Fire Tests Examining Sustainability, Smouldering, And Emissions,” in World Conference on Timber Engineering, Brisbane, 2025.

[8] L. Hasburgh, K. Bourne and D. Barber, “Determination Of Char Rates For Glulam Columns Exposed To A Standard Fire For Three Hours,” in World Conference on Timber Engineering, Santiago, 2020.

[9] D. Barber, E. Christensen, P. Kotsovinos, M. Heidari and J. Schulz, “Accounting For Post-Peak Compartment Temperature Thermal Degradation Of Mass Timber,” in World Conference on Timber Engineering, Oslo, 2023.

[10] H. A. Buchanan and K. A. Abu, Structural Design for Fire Safety, Chichester: John Wiley & Sons, Ltd, 2017.

[11] European Committee for Standardization, "Eurocode 5: Design of Timber Structures – Part 1-2: General – Structural Fire Design. EN 1995-1-2:2004.," CEN, Brussels, 2004.

[12] American Wood Council, National Design Specification (NDS) for Wood Construction with Commentary: 2018 Edition, Leesburg, VA: American Wood Council, 2018.